**Distribution Agreement**

In presenting this thesis as a partial fulfillment of the requirements for a degree from Emory University, I hereby grant to Emory University and its agents the non-exclusive license to archive, make accessible, and display my thesis in whole or in part in all forms of media, now or hereafter now, including display on the World Wide Web. I understand that I may select some access restrictions as part of the online submission of this thesis. I retain all ownership rights to the copyright of the thesis. I also retain the right to use in future works (such as articles or books) all or part of this thesis.

David Q. Trac April 11, 2013

# Rac1/Tiam1-mediated Nadph oxidase activation of epithelial sodium channels regulates neonatal lung aeration and alveolar development

by

David Q. Trac

My N. Helms, PhD

Adviser

Department of Biology

My N. Helms, PhD

Adviser

Amanda Starnes, DVM

Committee Member

William G. Kelly, PhD

Committee Member

2013

# Rac1/Tiam1-mediated Nadph oxidase activation of epithelial sodium channels regulates neonatal lung aeration and alveolar development

by

David Q. Trac

My N. Helms, PhD

Adviser

An abstract of
a thesis submitted to the Faculty of Emory College of Arts and Sciences
of Emory University in partial fulfillment
of the requirements of the degree of
Bachelor of Sciences with Honors

Department of Biology

2013

Abstract

Rac1/Tiam1-mediated Nadph oxidase activation of epithelial sodium channels regulates neonatal lung aeration and alveolar development

By David Q. Trac

Preterm infants have higher incidence of respiratory failure than term infants. These respiratory disorders are caused in part by delayed clearance of lung fluid. At birth, lung fluid clearance and aeration are mediated by active salt and water transport by epithelial sodium channel (ENaC) activity. Our lab has shown that oxidative environments can enhance ENaC activity, most likely via Nadph oxidase (Nox)-mediated O2- release. In this highly regulated process, we have shown that the small G-protein Rac1 plays an important role upstream of Nox signaling. However, the Rac1-guanine nucleotide exchange factors (GEFs) involved in the neonatal Nox-ENaC signaling process are unknown. Additionally, the role of ENaC in the postnatal developing lung has yet to be explored. Herein, we utilized real-time PCR and confocal immunohistochemistry to identify Tiam1 as the main GEF involved in the mediation of Rac1-activation of Nox and downstream ENaC activity. Additionally, we paired inhibitory drugs with morphological and functional analyses to elucidate a novel role for the Rac1/Tiam1-mediated Nox-ENaC signaling pathway in postnatal alveolar development.

# Rac1/Tiam1-mediated Nadph oxidase activation of epithelial sodium channels regulates neonatal lung aeration and alveolar development

by

David Q. Trac

My N. Helms, PhD

Adviser

A thesis submitted to the Faculty of Emory College of Arts and Sciences
of Emory University in partial fulfillment
of the requirements of the degree of
Bachelor of Sciences with Honors

Department of Biology

2013

Acknowledgements

We gratefully acknowledge the 2013 APS Writing and Reviewing for Journals workshop attended by DT.

Table of Contents

# Introduction

Preterm infants have a higher incidence of respiratory distress syndrome, transient tachypnea, and respiratory failure than term infants and are thus frequently admitted into neonatal ICU (17, 38). These respiratory disorders are characterized by a delayed lung fluid clearance as a result of a disruption in the transition of the fetal lung at birth from a fluid-secreting organ to an organ that can actively reabsorb salt and water.

Epithelial sodium channels (ENaC) have been shown to play a critical role in the adaptation of the newborn lung to air breathing. In fact, α-ENaC deficient mice have defective neonatal lung fluid clearance and die shortly after birth (23). ENaC transports sodium ions from the alveolar airway lumen into the cytosol, thereby generating the osmotic driving force for water reabsorption in the lung and subsequent resolution of lung edema. However, the exact signaling mechanisms governing ENaC activation at birth remain unclear, albeit oxygen signaling as the fetal lungs transition from low to high oxygen tension has been implicated in regulating lung ENaC (6, 32, 37, 39, 50, 54). In adult mouse alveolar type I (AT1) and type II (AT2) epithelial cells, we have shown that reactive oxygen species (ROS) generated by Rac1-mediated Nadph oxidase (Nox) activity play a key role in regulating ENaC, as illustrated in Figure 1 (46).

While ENaC activity and expression has been extensively characterized in the fetal lung (24, 31, 47), its role in the postnatal lung beyond fluid homeostasis remains undefined. From postpartum day 1 to postpartum day 20 (P1-P20), the mouse lung is primarily concerned with alveolar development (9). During this stage, we hypothesize that Nox oxidant signaling may be

responsible for regulating ENaC activity and triggering alveolar development. Several observations point to a developmental role for Nox oxidant signaling. Nox and ROS have been implicated in tissue regeneration, controlled apoptosis during development, and activation of vascular transcription factors and growth factors (21, 30, 41).

The purpose of this study is two-fold. We utilized real-time PCR and paired inhibitory drugs with morphological and functional analyses to investigate whether Rac1-mediated Nox oxidant signaling plays a key role in activating ENaC for lung aeration at birth and whether it may also then play a subsequent role in triggering alveolar development in the postnatal lung.

# Methods

## *Chemicals and reagents*

Unless otherwise stated, all chemicals and reagents were purchased from Sigma-Aldrich.

## *Primer design*

Primer pairs (Table 1) were purchased from Integrated DNA Technologies (Coralville, IA) and were designed to produce short amplicons (70-150 bp). For accurate data analysis, amplification efficiency of the primer pairs must be close to 100% (43). Amplification efficiency of each primer pairs was tested using a calibration curve (Figure 2). Primer specificity was evaluated with dissociation curve analysis.

## *Animal model*

All animal studies were performed in strict accordance with the recommendations in the Guide for the Care and Use of Laboratory Animals of the National Institutes of Health. The protocol was approved by the Emory University Institutional Animal Care and Use Committee. All surgery was performed under anesthesia with xylazine and ketamine, and all efforts were made to minimize suffering. Timed pregnant C57BL/6 mice were purchased from Charles River Laboratories (Wilmington, MA) at E11 or bred in-house.

For lung histology and morphology studies, naturally born C57BL/6 mouse litters were exposed to drug treatment—1 mM amiloride, a direct blocker of ENaC activity (26, 27); 100 µM NSC 23766, a specific inhibitor of Tiam1-mediated Rac1 activation (2, 19, 53); or 300 µM apocynin, an inhibitor of p47phox translocation and activation of Nox1-3 (7)—every two days, starting on postnatal day 1 up to postnatal day 15. Initially, pups were exposed to 5 µl of drug. Drug volume was increased by increments of 5 µl until P7, after which drug volume remained constant at 20 µl. Control pups were treated with corresponding volumes of PBS. This dose is proportional to doses previously used in our adult mouse studies (20, 46). To ensure proper delivery of the treatment to the alveoli, mouse pups were held upright and treatment solutions were placed using a P20 pipette on the pups' nostrils. After the treatment solutions were aspirated over the next 30-60 s, they were washed down with 5 µl of PBS, which were also applied over the nostrils and aspirated over the next 30-60 s.

For lung aeration studies, dams were delivered approximately 15 mg/kg/day of either the specific Rac1-inhibitor NSC 23766 or the pan-Nox inhibitor diphenyleneiodonium (DPI) from embryonic day 17 to embryonic day 20 (E17-E20) via their drinking water. Drinking water was changed daily to maintain drug stability. At E20, dams were euthanized with an intraperitoneal overdose of xylazine/ketamine. Mouse litters were then delivered by caesarian section via midline laparotomy. Pup lung aeration was measured as described below.

*Neonatal primary AT2 cell isolation and culture*

Primary alveolar type II cells were isolated from neonatal pup lungs for immunohistochemistry and confocal microscopy. First, P1 pups were anesthetized with an intraperitoneal injection of xylazine/ketamine and euthanized by exsanguination via the renal artery. Under a Zeiss Stemi 2000-C Stereo microscope, mouse pup lungs were lavaged three times with 30 µl PBS via a tracheal cannula to remove alveolar macrophages. Lungs were subsequently perfused via the pulmonary artery with PBS until blanch; the right and left atria were cut to relieve pressure. To digest lung tissue, lungs were instilled with dispase via the tracheal cannula until fully inflated (about 0.3 ml dispase). The trachea was then tied off and the lungs were removed *en bloc* and incubated at room temperature in 3 ml of dispase for 45 minutes. Afterwards, lung lobes were teased away from heart and bronchial tissue and minced in a 1:1 solution of neonatal calf serum (NCS) and 0.01% DNase 1 in mouse cell media (DMEM/F12 media with 10 mM HEPES, 0.04 mM L-glutamine, 1x MEM non-essential amino acids, and 1 mg/ml Primocin™). Cell suspension was sequentially filtered through a 100 µm and 40 µm filter before being seeded on poly-D-lysine round glass coverslips. Cells were left to adhere overnight in complete mouse cell media (mouse cell media with additional 0.25% BSA, 10 nM hydrocortisone, and 0.5% insulin-transferrin-sodium-selenite liquid media supplement).

*Cryosectioning and H&E staining*

On postnatal day 15, mouse pups were anesthetized with an intraperitoneal injection of xylazine/ketamine and euthanized by exsanguination via the renal artery. Lungs were then prepared for cryosectioning. First, lungs were perfused with PBS via the pulmonary artery until blanch and then uniformly inflated with Tissue-Tek OCT Compound (Sakura Finetek USA) via a

tracheal cannula. The lung and heart tissue was removed *en bloc* and embedded in OCT compound in cryomolds. Molds were dipped in liquid nitrogen to flash freeze the tissue. Rapid freezing reduces the formation of ice crystals and minimizes morphological damage. Samples were stored at -80°C until ready for sectioning. Tissues were cryosectioned using a Leica CM1520 cryostat (Leica Biosystems), available for use at the Image Analysis Core of the Digestive Dieseases Research Center at Emory University. 10 µm sections were fixed with acetone and stained with H&E for analysis of lung histology and morphology.

*Lung histology and morphology*

Lung alveolar morphology of H&E stained sections was visualized using an Olympus IX71 microscope and photomicrographs were captured using a camera attachment. Alveolar development was quantified by radial alveolar counts (RAC; a measure of the number of alveoli from the terminal bronchiole to the nearest connective tissue septum) and mean linear intercept (MLI; a measure of alveolar size). Increased alveolar development can be visually interpreted as an increase in septation and decrease in alveolar size. This correlates with larger RAC values and smaller MLI values. RAC measurements were gathered as described by Emery and Mithal (8, 13). A line perpendicular to the nearest connective tissue septum and intersecting the geometric center of a terminal bronchiole airway was drawn; RAC is given as the number of alveoli intersected by this line (Figure 3A). MLI measurements were gathered as described by Dunnill (18). Two traversing lines of equal length were drawn at right angles such that they intersected at their midpoints and then centered on the lung field (Figure 3B). MLI is given by the equation $MLI = \frac{N \cdot L}{m}$, where N is the number of traverses, L is the length of the traverse, and m is the total

number of intercepts by the traverses. A cut through an alveolar wall was counted as one intercept and a cut in or out of a blood vessel or airway was counted as half an intercept. Images from at least ten 100X lung fields were taken from each pup, consisting of a mixture of images from the apex, middle, and base of each lung. Lung fields were randomly selected such that each includes an alveolar duct or bronchiolar airway and a segment of the visceral pleura.

*Lung aeration measurements*

Lung function and aeration at birth were evaluated with wet:dry lung weight ratios. E20 mouse pups were delivered by caesarian section. Residual amniotic fluid was cleaned off of their noses with gauze to stimulate breathing. They were monitored for 1 hour under a heat lamp to ensure proper and regular breathing. Afterwards, mouse pups were euthanized by swift decapitation. Lungs were removed *en bloc* and blotted to remove surface fluids. Heart tissue was trimmed away and the wet lung weight was measured. Dry lung weight was measured after lungs were dehydrated in a 100°C isotemp oven overnight.

*Immunohistochemistry and confocal microscopy*

Freshly cultured neonatal AT2 cells were incubated in primary rabbit anti-Tiam1 antibody (Santa Cruz) or primary rabbit anti-Arhgef7 antibody (Cell Signaling) diluted 1:100 followed by incubation in secondary anti-rabbit IgG antibody conjugated to Alexa Fluor 488 (Invitrogen) diluted 1:20,000 in PBS containing 1% BSA and 1X sodium azide. Lysotracker Red (LTR, Invitrogen) was used per manufacturer protocol to mark lysosomes commonly found in AT2

cells. Co-localization with α-ENaC was studied by incubating cells in primary goat anti-α-ENaC C-20 antibody (Santa Cruz) diluted 1:100 followed by incubation in secondary anti-goat IgG antibody conjugated to Alexa Fluor 568 (Invitrogen) diluted 1:20,000 in PBS containing 1% BSA and 1X sodium azide; LTR dye was not used. Cells were then fixed in 4% paraformaldehyde and mounted in VECTASHIELD HardSet mounting medium with 4'6'diamidino-2-phenylindole (DAPI, Vector Laboratories). Confocal imaging was conducted at the Emory-Children's Pediatric Research Cell Imaging Core using an Olympus FV1000 confocal laser scanning microscope.

*mRNA analysis*

Transcript levels of genes of interest were measured by quantitative real-time PCR. RNA samples were prepared from mouse pups at P1, P2, P3, P4, P5, and P7. Mouse pups were anesthetized with an intraperitioneal injection of xylazine/ketamine and euthanized by exsanguination via the renal artery. Mouse pup lungs were lavaged three times with 30 µl PBS via a tracheal cannula to remove alveolar macrophages, then perfused with PBS until blanch, and removed *en bloc*. Heart and connective tissue were trimmed away. Total RNA was extracted from whole lungs using TRIzol (Invitrogen) and column-purified using the RNeasy isolation kit (Qiagen) per manufacturer protocol. RNA was treated was DNase 1 and reverse transcribed using Superscript II RNaseH-reverse transcriptase (Invitrogen). Primer pairs used in the PCR reaction are listed in Table 1. Cycle threshold (Ct) levels of mRNA expression were normalized to mouse GAPDH levels and are expressed as $2^{-\Delta Ct}$.

*Statistical analysis*

Data are reported as means ± SE. Multiple comparisons were performed using one-way ANOVA followed by Scheffe's post-hoc test. Trends in developmental gene expression were analyzed with linear regression. All statistical analysis was performed using Statistical Analysis System (SAS 9.3) software. Results were considered significant if $P < 0.05$.

# Results

## *Rac1-GEF, Nox, and ENaC transcript expression during postnatal mouse lung development*

Our lab has shown that oxidative environments can enhance ENaC activity, most likely via Nadph oxidase (Nox)-mediated O2- release (20). In this highly regulated process, we have shown that the small G-protein Rac1 plays an important role upstream of Nox signaling. Guanine nucleotide exchange factors (GEFs) are required to activate Rac1 by stimulating the release of GDP to allow binding of GTP. However, the Rac1-GEFs involved in the Nox-ENaC signaling process remain unknown. Using real-time PCR, we examined the expression of a subset of Rac1-GEFs in neonatal mouse lung: Arhgef7, Sos1, Sos2, Rasgrf2, and Tiam1. In Figure 4, we show that Arhgef7, Sos1, Sos2, Rasgrf2, and Tiam1 transcript levels are all expressed in neonatal mouse lung and all increase steadily in a linear fashion from postnatal day 1 to postnatal day 7 ($P < 0.05$). Arhgef7 transcript expression is highest, followed by Sos1 > Sos2 ≈ Rasgrf2 > Tiam1. Interestingly, GEF transcript expression in adult (12 week) mouse lungs is down-regulated compared to expression in P7 mouse lungs, suggesting an important role for GEFs in postnatal lung development.

Activated Rac1-GTP mediates the proper assembly of Nox cytoplasmic subunits p40phox, p67phox, and p47phox to regulate Nox1-3 activity. While Nox1 and Nox3 transcript levels remain unchanged between P1 and P7 (Figures 5A and 5C), Nox2 transcript levels increase linearly (Figure 5B). Transcript levels of Nox4, whose activity is not mediated by Rac1, also increase linearly (Figure 5D). Nox4 transcript expression is highest, followed by Nox2 > Nox1 ≈

Nox3. Interestingly, the increase in Nox2 and Nox4 transcript levels is independent of p22phox and p47phox transcript levels (Figures 5E and 5F).

Transcript levels of α-, β-, and γ-ENaC remain unchanged from P2 to P7, but are significantly elevated at P1 ($P < 0.05$) (Figure 6). As expected, α-ENaC expression is highest, followed by γ-ENaC > β-ENaC.

*Tiam1, but not Arhgef7, co-localizes with α-ENaC in isolated alveolar type II cells*

In determining specifically which Rac1-GEF may be involved in the Nox-ENaC signaling process found in alveolar epithelial cells, we focused on Arhgef7 and Tiam1. If Arhgef7 or Tiam1 is involved in the Nox-ENaC signaling pathway, then we would expect immunolabeled Arhgef7 or Tiam1 to co-localize with immunolabeled α-ENaC in fluorescence microscopy. While both Arhgef7 and Tiam1 are expressed in P1 AT2 cells (Figures 7A-D and 8A-D), only Tiam1 co-localizes with α-ENaC (Figures 8E-F). Subsets of the z-axis show that Tiam1/α-ENaC co-localization signal (a yellow-orange fluorescence) is mainly found near the cellular membrane, ENaC's site of activity, and not in the cytoplasm. Immunolabeled Arhgef7 exhibits minimal co-localization with immunolabeled α-ENaC (Figures 7E-F). In fact, Arhgef7 expression in AT2 cells seems to be lower compared to Tiam1 expression. These data suggest that Tiam1 is the key GEF involved in the Nox-ENaC signaling pathway during the postnatal lung stage.

*NSC 23766 and apocynin cause a tendency towards lung fluid attenuation at birth*

While it has been shown that ENaC activity plays a major role in lung fluid clearance and aeration at birth (23), the mechanisms that regulate ENaC upregulation and activity at this critical stage have yet to be elucidated. Our lab has shown that Rac1-mediated Nox superoxide ($O_2^-$) release regulates ENaC in adult mouse alveolar epithelial cells (20, 46). To investigate whether this pathway plays a role in ENaC activation at birth, mouse pups were exposed to NSC 23766 or DPI from E17-E20 *in utero*. If Rac1-mediated Nox activates ENaC at birth, then we would expect to see fluid attenuation and thus a higher wet:dry lung weight ratio in NSC 23766 or DPI treated pups compared to vehicle-exposed pups. Indeed, in our preliminary studies, we show that mouse litters exposed to Rac1-inhibitor or DPI exhibited seemingly higher wet:dry lung weight ratios than vehicle-exposed (Figure 9). It is interesting to note that pups exposed to Rac1-inhibitor or DPI *in utero* were more lethargic than vehicle-exposed pups. Additionally, in both treatment groups, one of the pups was stillborn, whereas all vehicle-exposed pups were delivered healthy.

*NSC 23766, apocynin, and amiloride administration inhibit postnatal lung development.*

While ENaC has been studied extensively in the fetal and early postnatal lung (24, 31, 47), ENaC's role in the postnatal developing stages of the lung remains unknown. In Figure 10E, we show that mice exposed to amiloride exhibit reduced septation and increased alveolar size, indicative of impaired lung development, compared to vehicle-exposed control mice. Mice that were exposed to NSC 23766 and apocynin also exhibited similar morphologies indicative of impaired lung development (Figure 10C and 10D). Quantitative analysis shows that mice

exposed to NSC 23766, apocynin, or amiloride have significantly reduced RAC and increased MLI (Figures 11A and 11B). These data suggest that the Rac1-mediated Nox-ENaC pathway plays a key role in postnatal alveolar development.

# Discussion

Major findings of this study include that Rac1-mediated Nadph oxidase regulation of epithelial sodium channel activity plays a key role in postnatal alveolar development. This observation, and others herein, have potential clinical implications and warrant additional discussion.

## *Tiam1-mediated Rac1 regulation of Nox2/Nox4 in the neonatal lung*

To date, the mechanisms that lead to ENaC activation in the neonatal lung remain unclear, albeit oxygen signaling as the fetal lungs transition from low to high oxygen tension has been implicated in regulating lung ENaC (6, 32, 37, 39, 50, 54). In our study, we provide support for a Nox-ENaC signaling pathway in neonatal mouse lung development (illustrated in Figure 12). Using fluorescence microscopy and NSC 23766, a specific inhibitor of Tiam1-mediated activation of Rac1, we show that Tiam1 is likely the main GEF involved in the mediation of Rac1 activation in this pathway (Figures 8, 10, and 11).

Nox2 and Nox4 transcript levels increase linearly with pup age, and are thus implicated in this developmental pathway (Figure 5B and 5D). Although Nox2 and Nox4 levels increase independently of the membrane stabilizing domain p22phox, Serrander et al. have shown that an increase in p22phox expression may not necessarily be needed for increased Nox4-ROS production and that Nox4 activity is independently determined by mRNA levels (45). In fact, siRNA mediated knockdown of p22phox has even been shown to increase Nox4 mRNA levels (33). Interestingly, although Nox4 transcript levels are 6-8 folds higher than Nox2 transcript

levels, blocking Rac1 activation of Nox2, by inhibiting the translocation of p47phox to the alveolar cell membrane with apocynin, effectively and sufficiently inhibits alveolar development (Figure 11). A possible explanation, then, for the high expression level of Nox4 may be Nox2 ROS-mediated activation of Nox4 ROS release; the abundant Nox4 may be required to amplify the oxidant signal generated by Nox2. This idea is in agreement with reports by Pendyala et. al. that show that Nox4 is redox sensitive and may be activated by ROS (33-35).

*ENaC's dual role in lung aeration and alveolar development*

ENaC plays a critical role in the adaptation of the newborn lung to air breathing. In fact, α-ENaC deficient mice die shortly after birth because of defective neonatal lung fluid clearance and aeration (23). While it is clear that ENaC activity is required at birth, ENaC's role in the postnatal developing stages of the lung remains unknown. In this study, we show that blocked ENaC activity causes lung fluid attenuation at birth and inhibits alveolar development between birth and P15 (Figures 9 and 11). This likely occurs via Rac1-mediation of Nox ROS release (illustrated in Figure 12). We also used real-time PCR to examine the expression profile of ENaC subunits. Classically, α-, β-, and γ-ENaC subunits in a fixed stoichiometry comprise epithelial sodium channels (36, 48). In Figure 6, we show that between P1 and P2, α-, β-, and γ-ENaC transcript levels are significantly reduced, after which point they remain unchanged. This pattern may point to a developmental switch from the early robust activity needed for lung fluid clearance and aeration to a basal level of activity for maintenance of fluid homeostasis and stimulation of alveolarization. In humans, alveolarization occurs between 36 weeks and 3 years (9). Dysregulation of ENaC expression and timing of this developmental switch may be a

mechanistic explanation for the increased incidence of chronic postnatal respiratory complications and mortality often observed in preterms during infancy (4, 5, 11, 22, 28, 29). Basal levels of ENaC protein expression and activity, despite low transcript expression, may be maintained by oxidative inactivation of the ubiquitin-like protein Nedd8 and subsequent inhibition of ENaC ubiquitination (15). We have also recently shown that ENaC activity may also be directly modified by ROS oxidation of thiol subgroups on the α-ENaC subunit (16). This observation is important, because α-ENaC is vital for sodium reabsorption (26).

*Nadph oxidase and bronchopulmonary dysplasia*

In the clinical setting, treatment for preterm neonates traditionally consists of high concentrations of oxygen and positive-pressure ventilation. Although recent advances in the acute care of premature infants has reduced the dependency on therapy with high concentrations of oxygen, oxidative damage is still a major contributor to the lung injury process leading to the development of bronchopulmonary dysplasia within hours to days of delivery (55). BPD is a debilitating chronic lung disease characterized by arrested structural development of the lung, including inhibition of septation and alveolarization (25). Normalization of lung development after preterm birth is elusive. Intervention therapies targeted at enhancing lung antioxidant capacity have not been successful. Treatment with superoxide dismutase failed to lower the incidence of BPD (14). In this current study, we show that Nadph oxidases play a key role in mouse postnatal alveolar development, most likely through regulation of ENaC activity (Figures 10D and 11). These new data support a contraindication for antioxidant therapies for preterm infants. Antioxidant therapies may in fact promote the development of BPD by blocking Nox

oxidant signaling and inhibiting alveolar development. Others have also observed the protective effects of Nox4 ROS release (21, 44). Given the important role of the Rac1-mediated Nox-ENaC pathway in regulating alveolar development, our data suggest that Tiam1, Rac1, Nox2/Nox4, and ENaC are likely to be key therapeutic targets with the capacity to reverse the symptoms of BPD and normalize postnatal lung development. Further research is necessary to determine both the mechanism through which Nadph oxidase and ENaC activity promote alveolarization and the exact timing of the developmental "switch" to alveolarization, so that more effective BPD interventions can be designed.

*Future direction*

For the remainder of this project, additional experiments will focus on substantiating the proposed pathway illustrated in Figure 12 with confocal microscopy and immunohistochemistry, as well as Amplex Red measurements of ROS generation, and exploring Smad protein as a possible mechanism by which Nox oxidant signaling stimulates alveolar development. Several observations make Smad protein an interesting mechanistic intermediate. Nox ROS release has been linked to Smad signaling and Smad3 null mutant mice exhibit arrested alveolarization (10, 40).

Additionally, we will further investigate Nadph oxidase and ENaC as therapeutic targets for normalizing postnatal alveolar development in a mouse model of BPD. To model BPD, mouse pups will be exposed to 85% $O_2$ from P1 to P28. Hyperoxia has been shown to inhibit septation and arrest alveolarization, causing a BPD phenotype (3). The optimal methods for providing

respiratory support to preterms at high risk of BPD, as well as the safe and optimal blood levels of oxygen and carbon dioxide, remain controversial (1, 12, 42, 49, 51, 52). Given that Nox and ENaC are amenable to pharmacological manipulation in the lung, they may provide alternative avenues for the safe management of BPD.

References

1. Supplemental Therapeutic Oxygen for Prethreshold Retinopathy Of Prematurity (STOP-ROP), a randomized, controlled trial. I: primary outcomes. Pediatrics 105: 295-310, 2000.

2. **Akbar H, Cancelas J, Williams DA, Zheng J, and Zheng Y.** Rational design and applications of a Rac GTPase-specific small molecule inhibitor. Methods in enzymology 406: 554-565, 2006.

3. **Alejandre-Alcazar MA, Kwapiszewska G, Reiss I, Amarie OV, Marsh LM, Sevilla-Perez J, Wygrecka M, Eul B, Kobrich S, Hesse M, Schermuly RT, Seeger W, Eickelberg O, and Morty RE.** Hyperoxia modulates TGF-beta/BMP signaling in a mouse model of bronchopulmonary dysplasia. American journal of physiology Lung cellular and molecular physiology 292: L537-549, 2007.

4. **Alexander GR, Kogan MD, and Himes JH.** 1994-1996 U.S. singleton birth weight percentiles for gestational age by race, Hispanic origin, and gender. Maternal and child health journal 3: 225-231, 1999.

5. **Allen MC, Alexander GR, Tompkins ME, and Hulsey TC.** Racial differences in temporal changes in newborn viability and survival by gestational age. Paediatric and perinatal epidemiology 14: 152-158, 2000.

6. **Baines DL, Ramminger SJ, Collett A, Haddad JJ, Best OG, Land SC, Olver RE, and Wilson SM.** Oxygen-evoked Na+ transport in rat fetal distal lung epithelial cells. The Journal of physiology 532: 105-113, 2001.

7. **Barbieri SS, Cavalca V, Eligini S, Brambilla M, Caiani A, Tremoli E, and Colli S.** Apocynin prevents cyclooxygenase 2 expression in human monocytes through NADPH oxidase

and glutathione redox-dependent mechanisms. Free radical biology & medicine 37: 156-165, 2004.

8. **Betz P, Nerlich A, Bussler J, Hausmann R, and Eisenmenger W.** Radial alveolar count as a tool for the estimation of fetal age. International journal of legal medicine 110: 52-54, 1997.

9. **Bourbon J, Boucherat O, Chailley-Heu B, and Delacourt C.** Control mechanisms of lung alveolar development and their disorders in bronchopulmonary dysplasia. Pediatric research 57: 38R-46R, 2005.

10. **Chen H, Sun J, Buckley S, Chen C, Warburton D, Wang XF, and Shi W.** Abnormal mouse lung alveolarization caused by Smad3 deficiency is a developmental antecedent of centrilobular emphysema. American journal of physiology Lung cellular and molecular physiology 288: L683-691, 2005.

11. **Clark R, Powers R, White R, Bloom B, Sanchez P, and Benjamin DK, Jr.** Prevention and treatment of nosocomial sepsis in the NICU. Journal of perinatology : official journal of the California Perinatal Association 24: 446-453, 2004.

12. **Collins MP, Lorenz JM, Jetton JR, and Paneth N.** Hypocapnia and other ventilation-related risk factors for cerebral palsy in low birth weight infants. Pediatric research 50: 712-719, 2001.

13. **Cooney TP and Thurlbeck WM.** The radial alveolar count method of Emery and Mithal: a reappraisal 2--intrauterine and early postnatal lung growth. Thorax 37: 580-583, 1982.

14. **Davis JM, Parad RB, Michele T, Allred E, Price A, and Rosenfeld W.** Pulmonary outcome at 1 year corrected age in premature infants treated at birth with recombinant human CuZn superoxide dismutase. Pediatrics 111: 469-476, 2003.

15. **Downs CA, Kumar A, Kreiner LH, Johnson NM, and Helms MN.** H2O2 Regulates Lung Epithelial Sodium Channel (ENaC) via Ubiquitin-like Protein Nedd8. The Journal of biological chemistry 288: 8136-8145, 2013.

16. **Downs CA, Trac DQ, Kreiner LH, Eaton AF, Johnson NM, Brown LA, and Helms MN.** Ethanol alters alveolar fluid balance via Nadph oxidase (NOX) signaling to epithelial sodium channels (ENaC) in the lung. PloS one 8: e54750, 2013.

17. **Dudell GG and Jain L.** Hypoxic respiratory failure in the late preterm infant. Clinics in perinatology 33: 803-830; abstract viii-ix, 2006.

18. **Dunnill MS.** Evaluation of a Simple Method of Sampling the Lung for Quantitative Histological Analysis. Thorax 19: 443-448, 1964.

19. **Gao Y, Dickerson JB, Guo F, Zheng J, and Zheng Y.** Rational design and characterization of a Rac GTPase-specific small molecule inhibitor. Proceedings of the National Academy of Sciences of the United States of America 101: 7618-7623, 2004.

20. **Goodson P, Kumar A, Jain L, Kundu K, Murthy N, Koval M, and Helms MN.** Nadph oxidase regulates alveolar epithelial sodium channel activity and lung fluid balance in vivo via O(-)(2) signaling. American journal of physiology Lung cellular and molecular physiology 302: L410-419, 2012.

21. **Hecker L, Vittal R, Jones T, Jagirdar R, Luckhardt TR, Horowitz JC, Pennathur S, Martinez FJ, and Thannickal VJ.** NADPH oxidase-4 mediates myofibroblast activation and fibrogenic responses to lung injury. Nature medicine 15: 1077-1081, 2009.

22. **Hulsey TC, Alexander GR, Robillard PY, Annibale DJ, and Keenan A.** Hyaline membrane disease: the role of ethnicity and maternal risk characteristics. American journal of obstetrics and gynecology 168: 572-576, 1993.

23. **Hummler E, Barker P, Gatzy J, Beermann F, Verdumo C, Schmidt A, Boucher R, and Rossier BC.** Early death due to defective neonatal lung liquid clearance in alpha-ENaC-deficient mice. Nature genetics 12: 325-328, 1996.

24. **Jain L and Eaton DC.** Physiology of fetal lung fluid clearance and the effect of labor. Seminars in perinatology 30: 34-43, 2006.

25. **Jobe AJ.** The new BPD: an arrest of lung development. Pediatric research 46: 641-643, 1999.

26. **Kelly O, Lin C, Ramkumar M, Saxena NC, Kleyman TR, and Eaton DC.** Characterization of an amiloride binding region in the alpha-subunit of ENaC. American journal of physiology Renal physiology 285: F1279-1290, 2003.

27. **Kemendy AE, Kleyman TR, and Eaton DC.** Aldosterone alters the open probability of amiloride-blockable sodium channels in A6 epithelia. The American journal of physiology 263: C825-837, 1992.

28. **Lemons JA, Bauer CR, Oh W, Korones SB, Papile LA, Stoll BJ, Verter J, Temprosa M, Wright LL, Ehrenkranz RA, Fanaroff AA, Stark A, Carlo W, Tyson JE, Donovan EF, Shankaran S, and Stevenson DK.** Very low birth weight outcomes of the National Institute of Child health and human development neonatal research network, January 1995 through December 1996. NICHD Neonatal Research Network. Pediatrics 107: E1, 2001.

29. **Lewis DF, Brody K, Edwards MS, Brouillette RM, Burlison S, and London SN.** Preterm premature ruptured membranes: a randomized trial of steroids after treatment with antibiotics. Obstetrics and gynecology 88: 801-805, 1996.

30. **Maulik N.** Reactive oxygen species drives myocardial angiogenesis? Antioxidants & redox signaling 8: 2161-2168, 2006.

31. **O'Brodovich H.** Epithelial ion transport in the fetal and perinatal lung. The American journal of physiology 261: C555-564, 1991.

32. **Otulakowski G, Duan W, Gandhi S, and O'Brodovich H.** Steroid and oxygen effects on eIF4F complex, mTOR, and ENaC translation in fetal lung epithelia. American journal of respiratory cell and molecular biology 37: 457-466, 2007.

33. **Pendyala S, Gorshkova IA, Usatyuk PV, He D, Pennathur A, Lambeth JD, Thannickal VJ, and Natarajan V.** Role of Nox4 and Nox2 in hyperoxia-induced reactive oxygen species generation and migration of human lung endothelial cells. Antioxidants & redox signaling 11: 747-764, 2009.

34. **Pendyala S, Moitra J, Kalari S, Kleeberger SR, Zhao Y, Reddy SP, Garcia JGN, and Natarajan V.** Nrf2 regulates hyperoxia-induced Nox4 expression in human lung endothelium: Identification of functional antioxidant response elements on the Nox4 promoter. Free Radical Biology and Medicine 50: 1749-1759, 2011.

35. **Pendyala S and Natarajan V.** Redox regulation of Nox proteins. Respiratory Physiology & Neurobiology 174: 265-271, 2010.

36. **Qadri YJ, Rooj AK, and Fuller CM.** ENaCs and ASICs as therapeutic targets. American journal of physiology Cell physiology 302: C943-965, 2012.

37. **Ramminger SJ, Baines DL, Olver RE, and Wilson SM.** The effects of PO2 upon transepithelial ion transport in fetal rat distal lung epithelial cells. The Journal of physiology 524 Pt 2: 539-547, 2000.

38. **Reese HC.** The Epidemiology of Respiratory Failure in Neonates Born at an Estimated Gestational Age of 34 Weeks or More. Journal of Perinatology 25: 251-257, 2004.

39. **Richard K, Ramminger SJ, Inglis SK, Olver RE, Land SC, and Wilson SM.** O2 can raise fetal pneumocyte Na+ conductance without affecting ENaC mRNA abundance. Biochemical and Biophysical Research Communications 305: 671-676, 2003.

40. **Rocic P and Lucchesi PA.** NAD(P)H oxidases and TGF-beta-induced cardiac fibroblast differentiation: Nox-4 gets Smad. Circulation research 97: 850-852, 2005.

41. **Sauer H and Wartenberg M.** Reactive oxygen species as signaling molecules in cardiovascular differentiation of embryonic stem cells and tumor-induced angiogenesis. Antioxidants & redox signaling 7: 1423-1434, 2005.

42. **Saugstad OD.** Oxygen for newborns: how much is too much? Journal of perinatology : official journal of the California Perinatal Association 25 Suppl 2: S45-49; discussion S50, 2005.

43. **Schmittgen TD and Livak KJ.** Analyzing real-time PCR data by the comparative C(T) method. Nature protocols 3: 1101-1108, 2008.

44. **Schroder K, Zhang M, Benkhoff S, Mieth A, Pliquett R, Kosowski J, Kruse C, Luedike P, Michaelis UR, Weissmann N, Dimmeler S, Shah AM, and Brandes RP.** Nox4 is a protective reactive oxygen species generating vascular NADPH oxidase. Circulation research 110: 1217-1225, 2012.

45. **Serrander L, Cartier L, Bedard K, Banfi B, Lardy B, Plastre O, Sienkiewicz A, Forro L, Schlegel W, and Krause KH.** NOX4 activity is determined by mRNA levels and reveals a unique pattern of ROS generation. The Biochemical journal 406: 105-114, 2007.

46. **Takemura Y, Goodson P, Bao HF, Jain L, and Helms MN.** Rac1-mediated NADPH oxidase release of O2- regulates epithelial sodium channel activity in the alveolar epithelium. American journal of physiology Lung cellular and molecular physiology 298: L509-520, 2010.

47. **Talbot CL, Bosworth DG, Briley EL, Fenstermacher DA, Boucher RC, Gabriel SE, and Barker PM.** Quantitation and localization of ENaC subunit expression in fetal, newborn, and adult mouse lung. American journal of respiratory cell and molecular biology 20: 398-406, 1999.

48. **Thibodeau PH and Butterworth MB.** Proteases, cystic fibrosis and the epithelial sodium channel (ENaC). Cell and tissue research 351: 309-323, 2013.

49. **Thome UH and Carlo WA.** Permissive hypercapnia. Seminars in neonatology : SN 7: 409-419, 2002.

50. **Thome UH, Davis IC, Nguyen SV, Shelton BJ, and Matalon S.** Modulation of sodium transport in fetal alveolar epithelial cells by oxygen and corticosterone. American journal of physiology Lung cellular and molecular physiology 284: L376-385, 2003.

51. **Tin W.** Oxygen therapy: 50 years of uncertainty. Pediatrics 110: 615-616, 2002.

52. **Tin W and Wariyar U.** Giving small babies oxygen: 50 years of uncertainty. Seminars in neonatology : SN 7: 361-367, 2002.

53. **Veluthakal R, Madathilparambil SV, McDonald P, Olson LK, and Kowluru A.** Regulatory roles for Tiam1, a guanine nucleotide exchange factor for Rac1, in glucose-stimulated insulin secretion in pancreatic beta-cells. Biochemical pharmacology 77: 101-113, 2009.

54. **Venkatesh VC and Katzberg HD.** Glucocorticoid regulation of epithelial sodium channel genes in human fetal lung. The American journal of physiology 273: L227-233, 1997.

55. **Welty SE.** Is there a role for antioxidant therapy in bronchopulmonary dysplasia? The Journal of nutrition 131: 947S-950S, 2001.

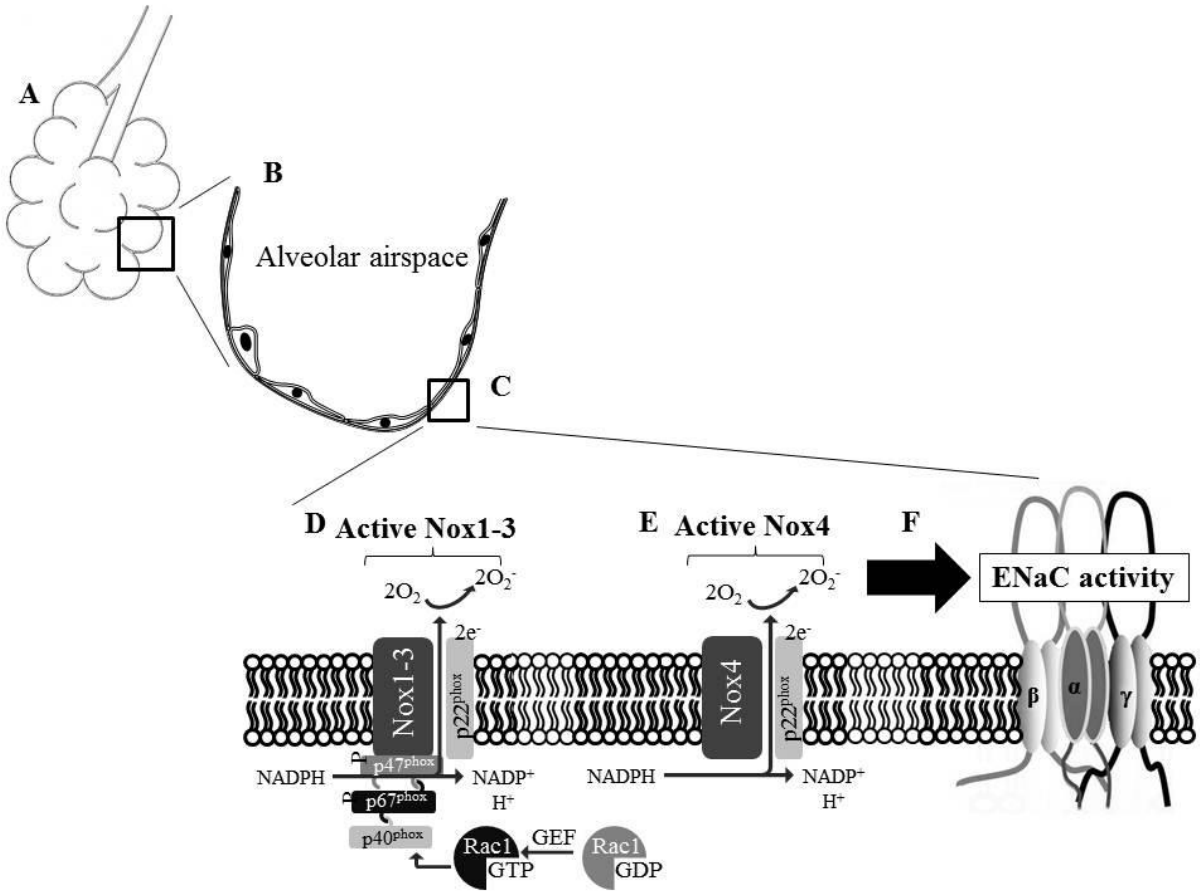


*Figure 1. Diagram of the Rac1-Nox-ENaC signaling pathway in alveolar epithelial cells.*

*A:* Alveolar structures at a terminal bronchiole. *B:* The alveolar epithelium consists of 95% alveolar type 1 and 5% alveolar type 2 epithelial cells, by surface area. *C:* Nox1-4 and ENaC are found on the membranes of both AT1 and AT2 cells. *D:* The activation of Nox1-3 is mediated by the proper assembly of cytoplasmic subunits p40phox, p47phox, and p67phox by Rac1-GTP. Guanine nucleotide exchange factors (GEFs) are required to activate Rac1 by stimulating the release of GDP to allow binding of GTP. *E:* The activation of Nox4, on the other hand, is independent of cytoplasmic subunits and only requires the association with the stabilizing domain, p22phox. *F:* Active Nox complexes produce superoxide ($O_2^-$), which can act as an oxidant signal for the activation of epithelial sodium channels (ENaC).

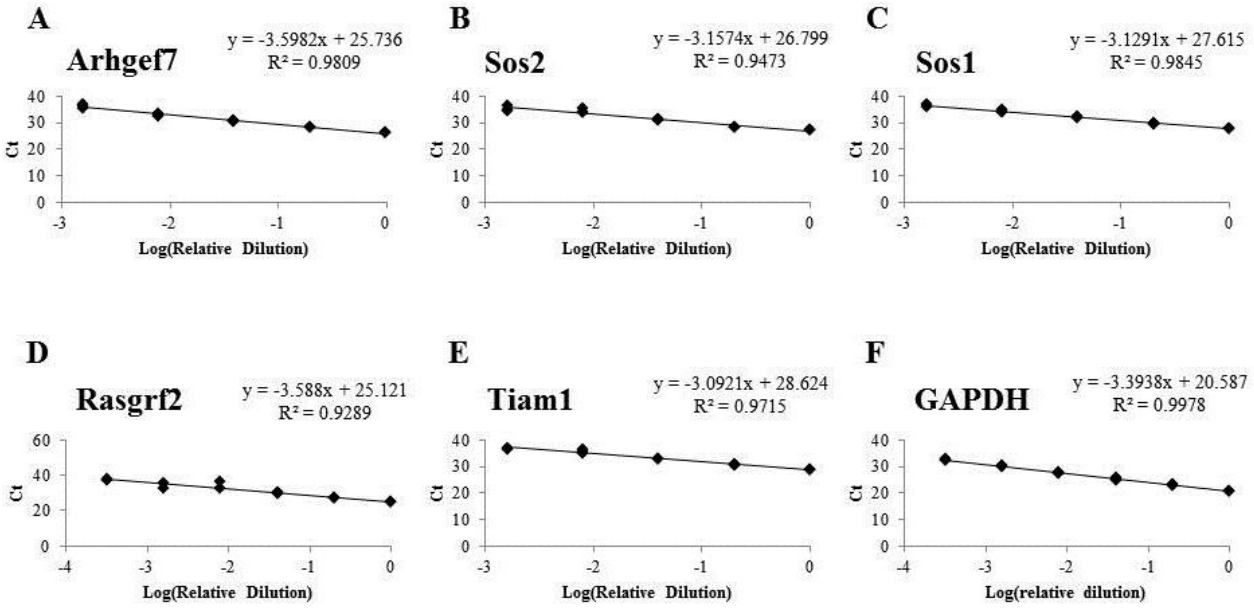


*Figure 2. Primer pair amplification efficiencies.*

Serial dilutions of a template of known concentration were amplified by primer pairs. Cycle threshold values (Ct) were graphed against template concentration expressed as log(relative dilution). The closer the slope is to -3.3, the closer the amplification efficiency is to 100%. ENaC primer pairs, Nox primer pairs, and Nox cytoplasmic subunit primer pairs were also similarly tested for amplification efficiency (data not shown).

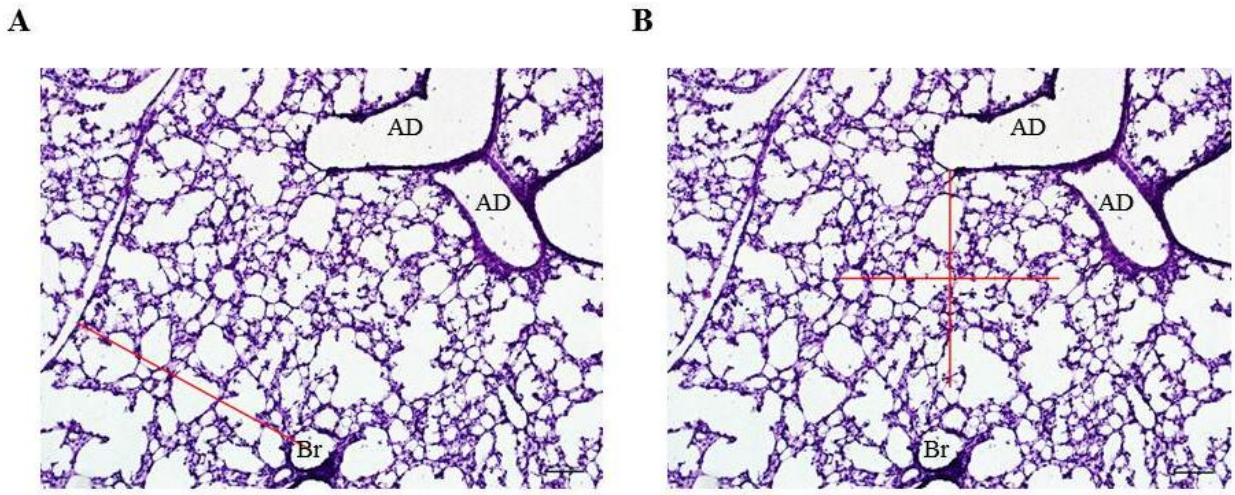


*Figure 3. Methods for MLI measurements and RAC measurements.*

*A:* Example of a perpendicular line drawn from lung epithelial perimeter to the geometric mean of a bronchiolar airway. RAC is given by the number of alveoli intercepted by this line. *B:* Example of transverse lines used to calculate MLI. The number of intercepts is given by the number of alveolar walls cut by the transverse crosshairs. (H&E stain, calibration bar = 100 µm, 100X magnification). Br, bronchiole. AD, alveolar duct.

*Table 1. Primer sequences.*

| | |
|---|---|
| **Rac-GEFs** | |
| Arhgef7-F | 5'- ACCTCGCTTACTGTGCCAACCA -3' |
| Arhgef7-R | 5'- GTACTTGTCCAGGCGCATGAAG -3' |
| Sos2-F | 5'- CACCAGTGGAATGGCACATCAG -3' |
| Sos2-R | 5'- CTTTGGTCCAGACACTCCCTAC -3' |
| Sos1-F | 5'- CAACATACAGGTCCTTTTGCAGAC -3' |
| Sos1-R | 5'- TGCGATCAGCTTCTGTTGGCTC -3' |
| Rasgrf2-R | 5'- GAGAACTTGCGACAGAGACGTG -3' |
| Rasgrf2-F | 5'- GCCTTTCACCTCCATTCCTGTC -3' |
| Tiam1-F | 5'- CCACATTGAGAAGTCAGACGCG -3' |
| Tiam1-R | 5'- CGGTTTCCTTGACACTGTTCACG -3' |
| **Nox isoforms** | |
| Nox1-F | 5’- CAG TTA TTC ATA TCA TTG CAC ACC TAT -3’ |
| Nox1-R | 5’- CAG AAG CGA GAG ATC CAT CCA -3’ |
| Nox2-F | 5’- CAG GAA CCT CAC TTT CCA TAA GAT -3’ |
| Nox2-R | 5’- AAC GTT GAA GAG ATG TGC AAT TGT -3’ |
| Nox3-F | 5’- GCT GGC TGC ACT TTC CAA AC -3’ |
| Nox3-R | 5’- AAG GTG CGG ACT GGA TTG AG -3’ |
| Nox4-F | 5’- CCC AAG TTC CAA GCT CAT TTC C -3’ |
| Nox4-R | 5’- TGG TGA CAG GTT TGT TGC TCC T -3’ |
| **Nox subunits** | |
| p22phox-F | 5’- AAC GAG CAG GCG CTG GCG TCC G -3’ |
| p22phox-R | 5’- GCT TGG GCT CGA TGG GCG TCC ACT -3’ |
| p47phox-F | 5’- CCA CAC CTG CTG GAC TTC TT -3’ |

| | |
|---|---|
| p47phox-R | 5’- ATC TTT GGG CAC CAG GTA TG -3’ |

**ENaC subunits**

| | |
|---|---|
| α-ENaC-F | 5’- TGC TCC TGT CAC TTC AGC AC -3’ |
| α-ENaC-R | 5’- CCC CTT GCT TAG CCT GTT C -3’ |
| β-ENaC-F | 5’- CCC CTG ATC GCA TAA TCC TA -3’ |
| β-ENaC-R | 5’- GCC CCA GTT GAA GAT GTA GC -3’ |
| γ-ENaC-F | 5’- ACC CTT TCA TCG AAG ACG TG -3’ |
| γ-ENaC-R | 5’- CCT CTG TGC ACT GGC TGT AA -3’ |

**Reference Gene**

| | |
|---|---|
| GAPDH-F | 5’- CAA GGT CAT CCA TGA CAA CTT TG -3’ |
| GAPDH-R | 5’- GGC CAT CCA CAG TCT TCT GG -3’ |

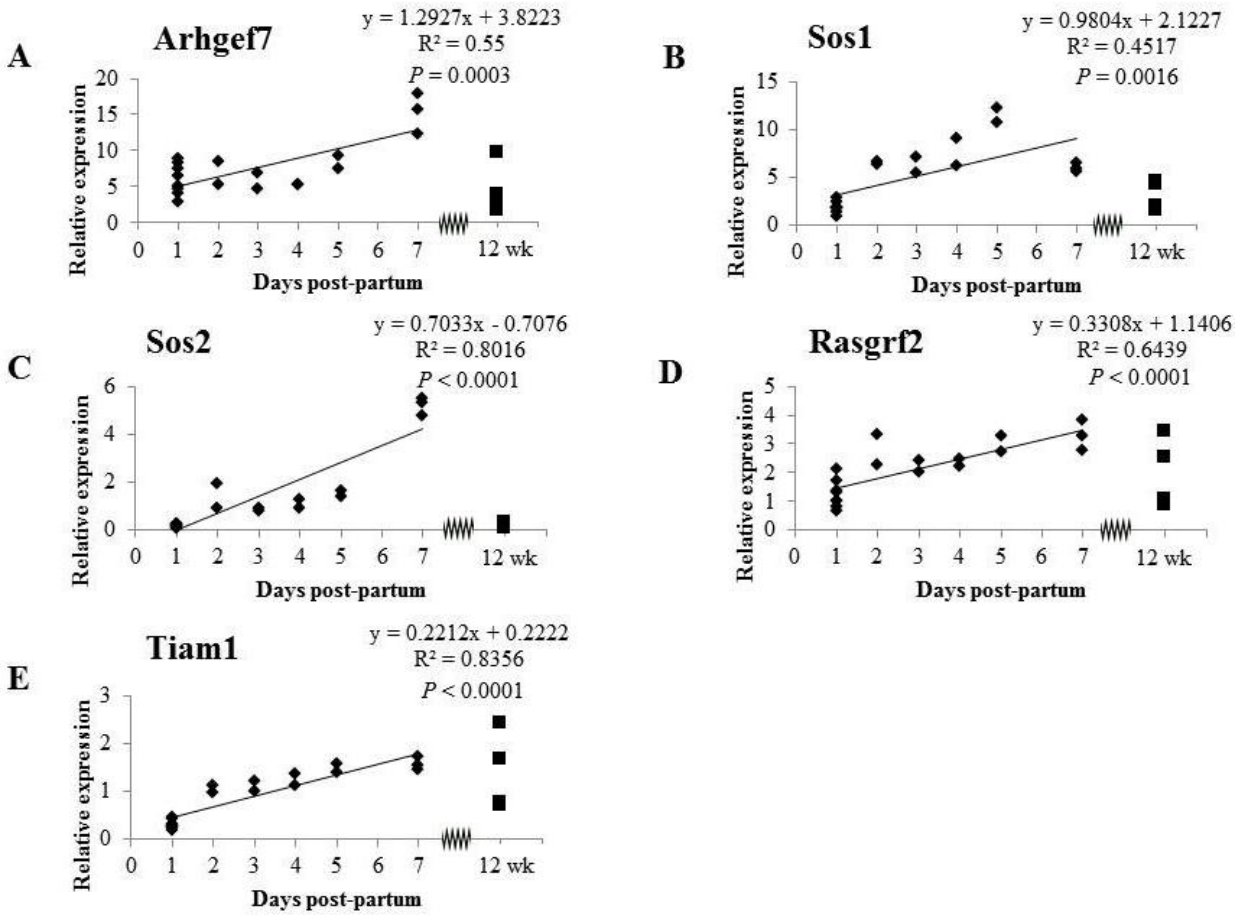


*Figure 4. Rac1-GEF transcript expression increases during postnatal lung development.*

*A-E:* Normalized Arhgef7, Sos1, Sos2, Rasgrf2, and Tiam1 mRNA levels increase linearly and significantly in mouse pup lung during development from P1 to P7. Data represents a total *N* of 19 (*N* = 8 for the P1 age group, *N* = 2 for groups P2 through P5, and *N* = 3 for the P7 age group). Normalized mRNA levels of adult (12 week) mouse lung are shown for comparison; *N* = 4.

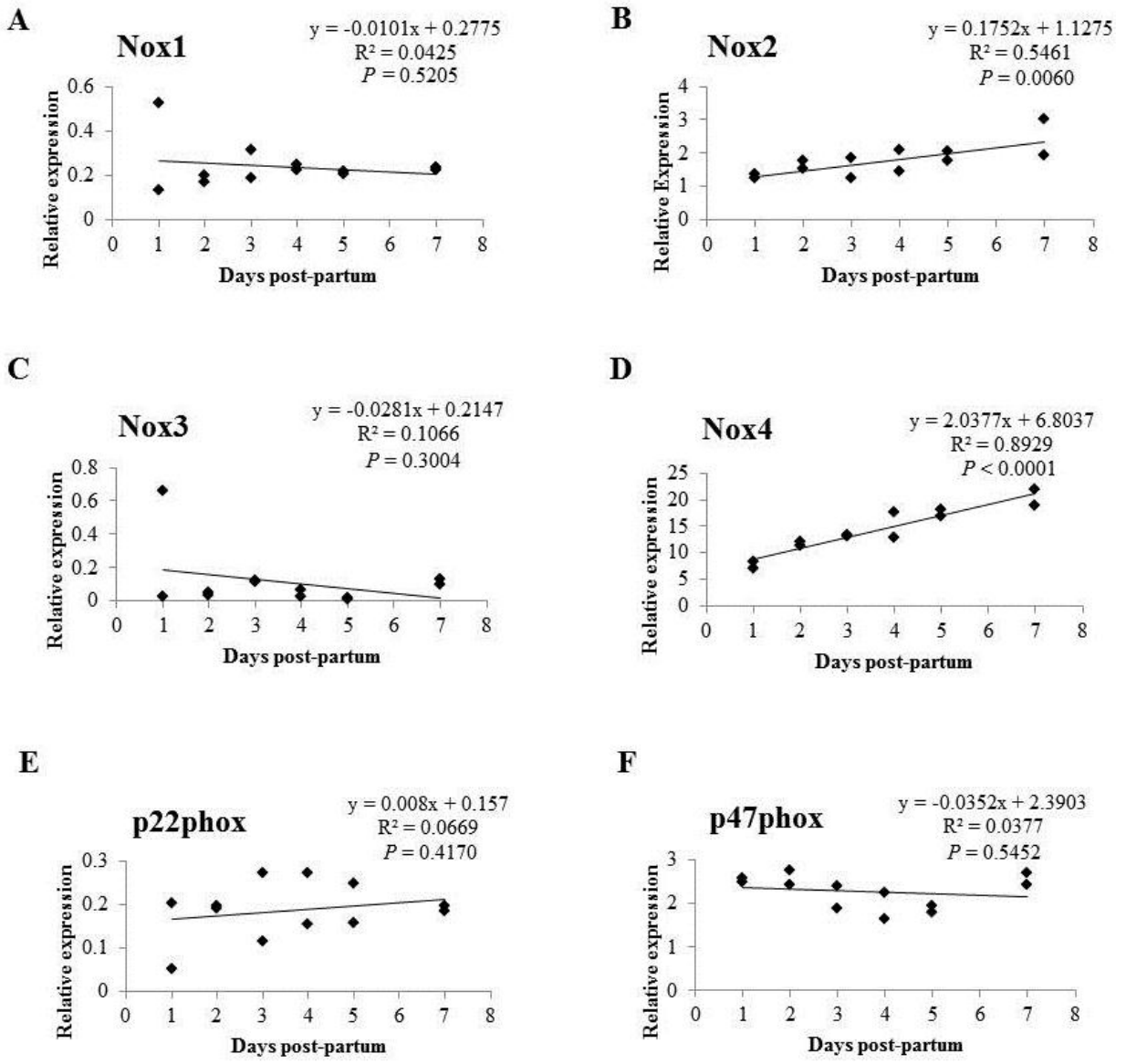


*Figure 5. Nox catalytic subunit and cytoplasmic subunit expression during postnatal lung development.*

*A-F:* Normalized Nox catalytic subunit (Nox1, Nox2, Nox3, and Nox4) and cytoplasmic subunit (p22phox and p47phox) mRNA levels are representative of a total *N* of 12 (*N* = 2 for each age group). Linear relationships are considered significant if $P < 0.05$.

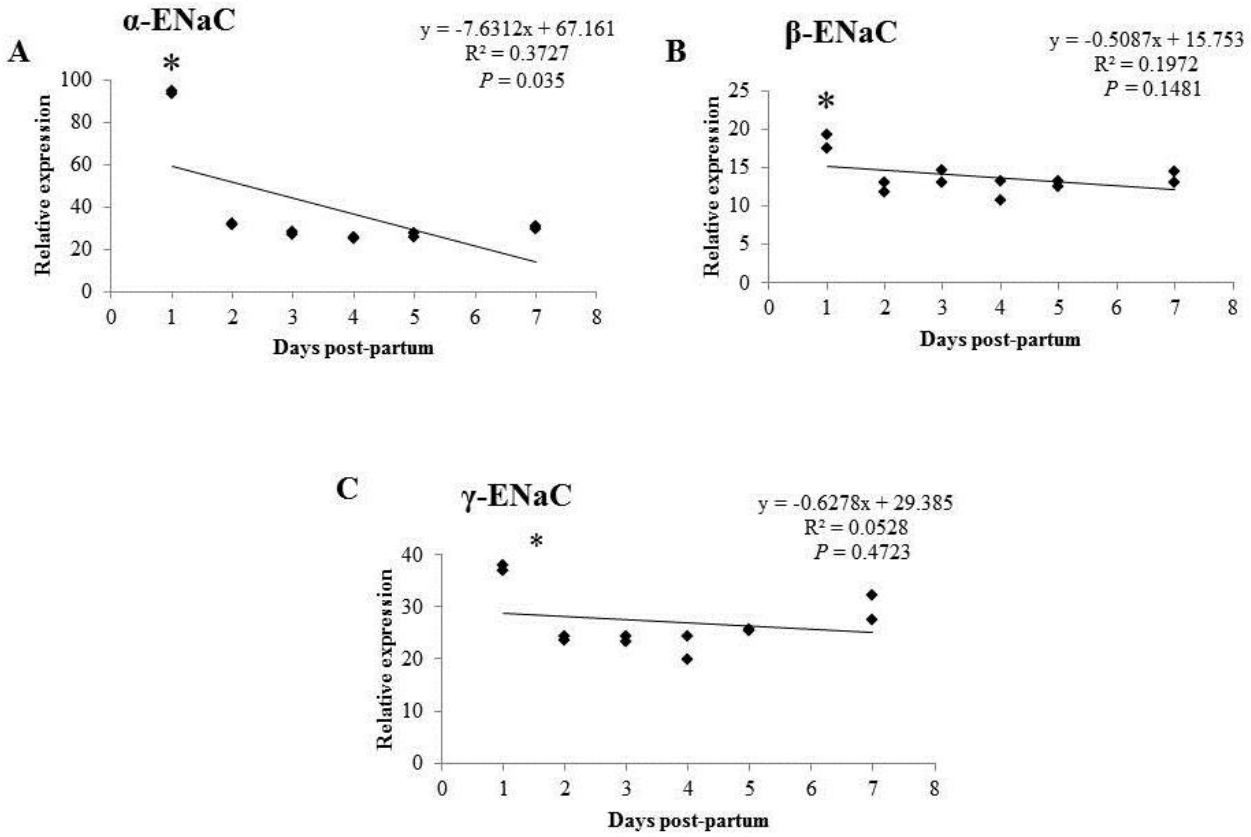


*Figure 6. ENaC subunit expression during postnatal lung development.*

*A-C:* Normalized α-ENaC, β-ENaC, γ-ENaC mRNA levels do not exhibit a significant linear relationship with mouse pup age. Data represents a total N of 12 (N = 2 for each age group). *$P < 0.05$.

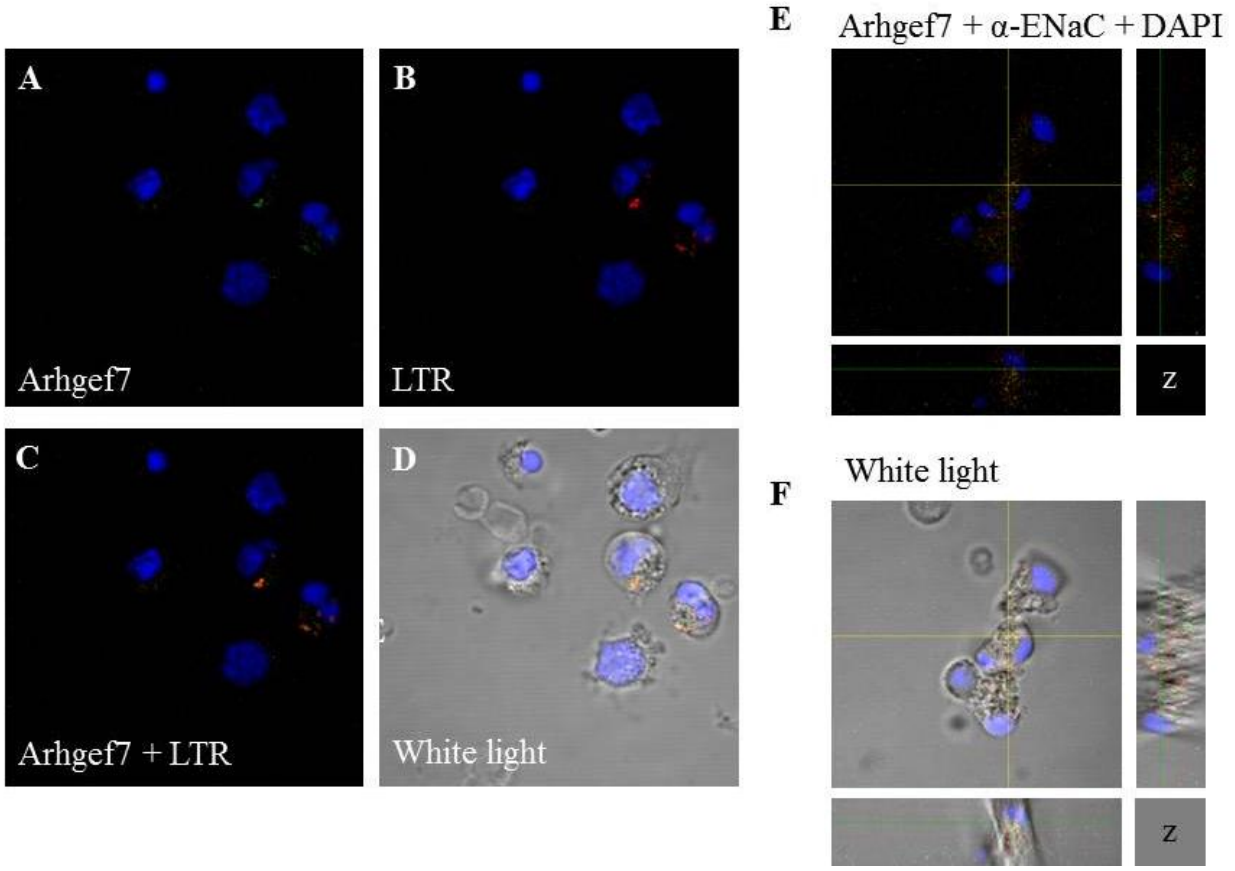


*Figure 7. Arhgef7 and α-ENaC expression in isolated alveolar type II cells.*

*A-D:* Anti-Arhgef7 antibody detected using Alexa Fluor 488 conjugated antibody (488/519 nm; green fluorescence); nuclei were stained with DAPI (350/470 nm; blue fluorescence); and AT2 cells were marked with Lysotracker Red (577/590 nm; red fluorescence). *A:* Arhgef7 localization relative to DAPI stained nuclei. *B:* Lysotracker Red marks lysosomes in AT2 cells. *C:* Arhgef7 expression is found in AT2 cells, as identified by Lysotracker Red. *D:* White light image of cells with Arhgef7 and Lysotracker Red labeling. *E-F:* Anti-Arhgef7 antibody detected using Alexa Fluor 488 conjugated antibody (488/519 nm; green fluorescence); anti-α-ENaC detected using Alexa Fluor 568 (578/603 nm; red fluorescence); and nuclei were stained with DAPI (350/470 nm; blue fluorescence). Subsets represent z-axis obtained from horizontal and vertical regions as

indicated. *E:* Arhgef7 localization relative to α-ENaC. *F:* Corresponding white light image with Arhgef7 and α-ENaC labeling.

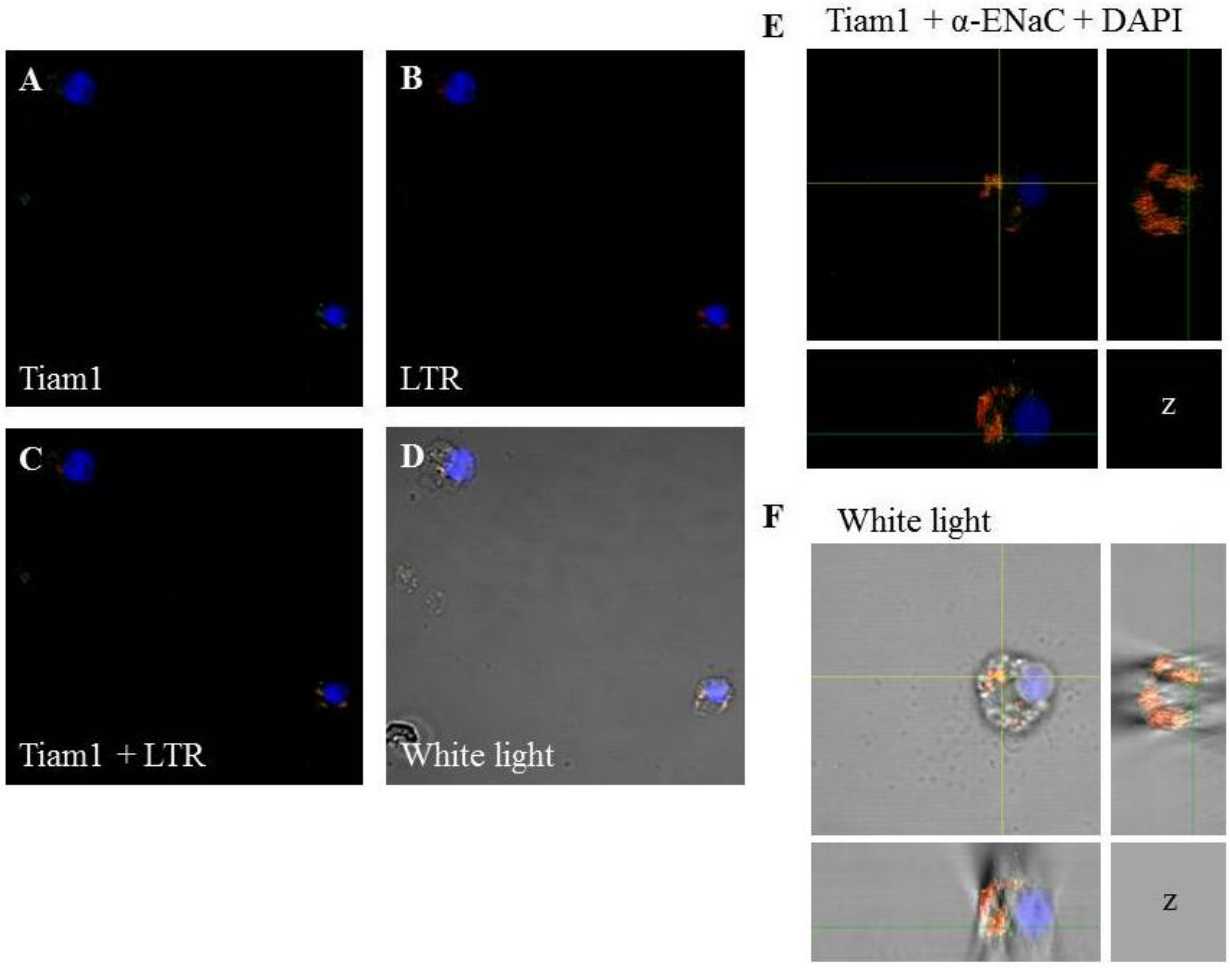


*Figure 8. Tiam1 and α-ENaC expression in isolated alveolar type II cells.*

*A-D:* Anti-Tiam1 antibody detected using Alexa Fluor 488 conjugated antibody (488/519 nm; green fluorescence); nuclei were stained with DAPI (350/470 nm; blue fluorescence); and AT2 cells were marked with Lysotracker Red (577/590 nm; red fluorescence). *A:* Tiam1 localization relative to DAPI stained nuclei. *B:* Lysotracker Red marks lysosomes in AT2 cells. *C:* Tiam1 expression is found in AT2 cells, as identified by Lysotracker Red. *D:* White light image of cells with Tiam1 and Lysotracker Red labeling. *E-F:* Anti-Tiam1 antibody detected using Alexa Fluor 488 conjugated antibody (488/519 nm; green fluorescence); anti-α-ENaC detected using Alexa Fluor 568 (578/603 nm; red fluorescence); and nuclei were stained with DAPI (350/470 nm; blue

fluorescence). Subsets represent z-axis obtained from horizontal and vertical regions as indicated. *E:* Tiam1 co-localizes with α-ENaC on the alveolar membrane. Pixels containing both red and green fluorescence contributions produce various shades of yellow to orange that indicate co-localization. *F:* Corresponding white light image with Tiam1 and α-ENaC co-localization on the alveolar membrane.

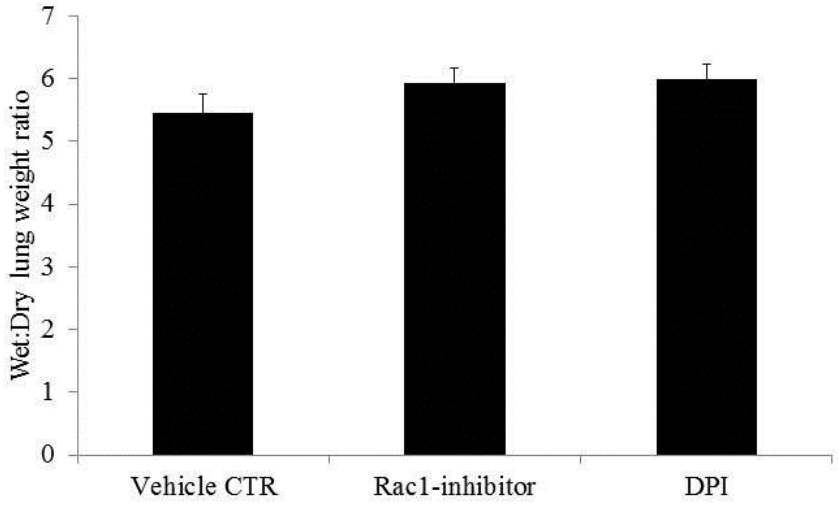


*Figure 9. Wet:dry lung weight ratios demonstrate lung function at birth.*

In our preliminary studies, wet:dry lung weight ratios measured from P1 mouse pups exposed to NSC 23766, a Rac1-inhibitor, or DPI, a pan-Nox inhibitor, *in utero* are seemingly increased compared to vehicle-exposed control.

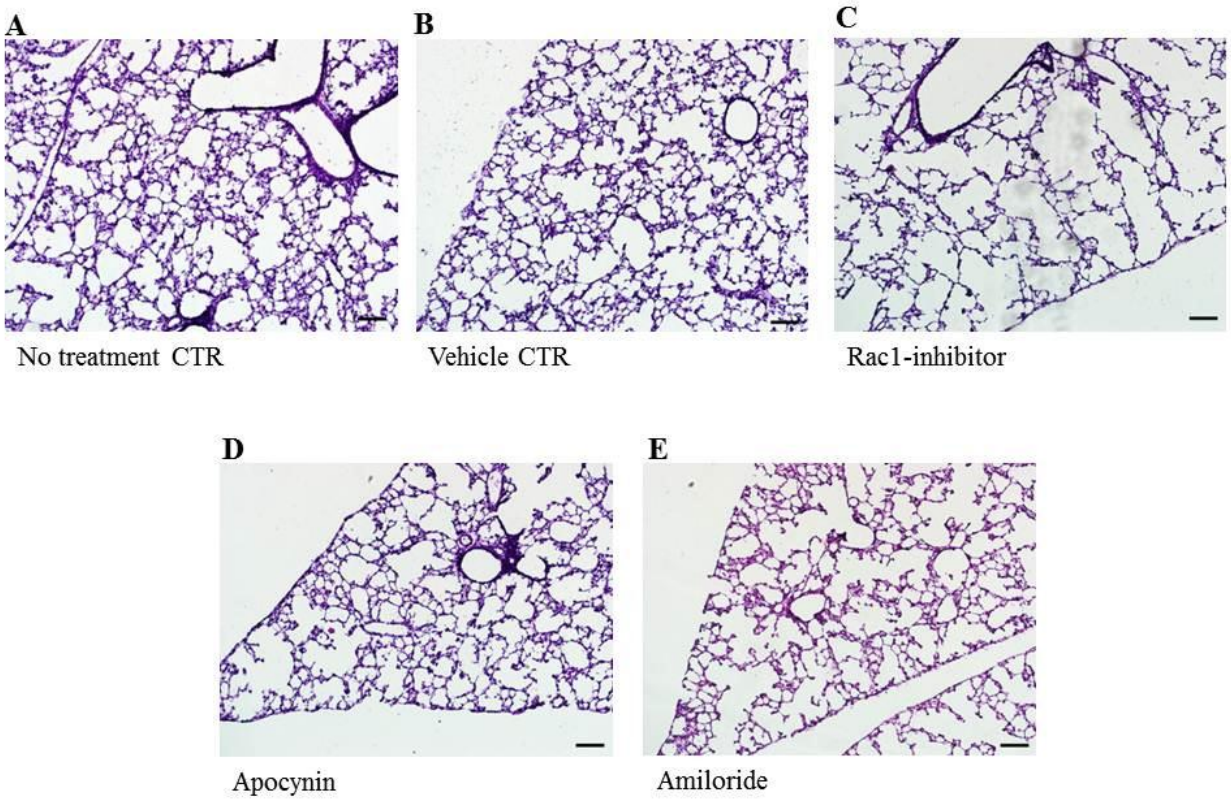


*Figure 10. Lung alveolarization in mouse pups exposed to ENaC, Rac1, and Nox inhibitors.*

*A-E:* Representative photomicrographs from P15 mouse pups exposed to no treatment (*A*); vehicle *(B)*; apocynin, an inhibitor of Nox activity (*C*); NSC 23766, an inhibitor of Rac1 activity (*D*); or amiloride, an inhibitor of ENaC activity (*E*). (H&E stain, calibration bar = 100 µm, 100X magnification).

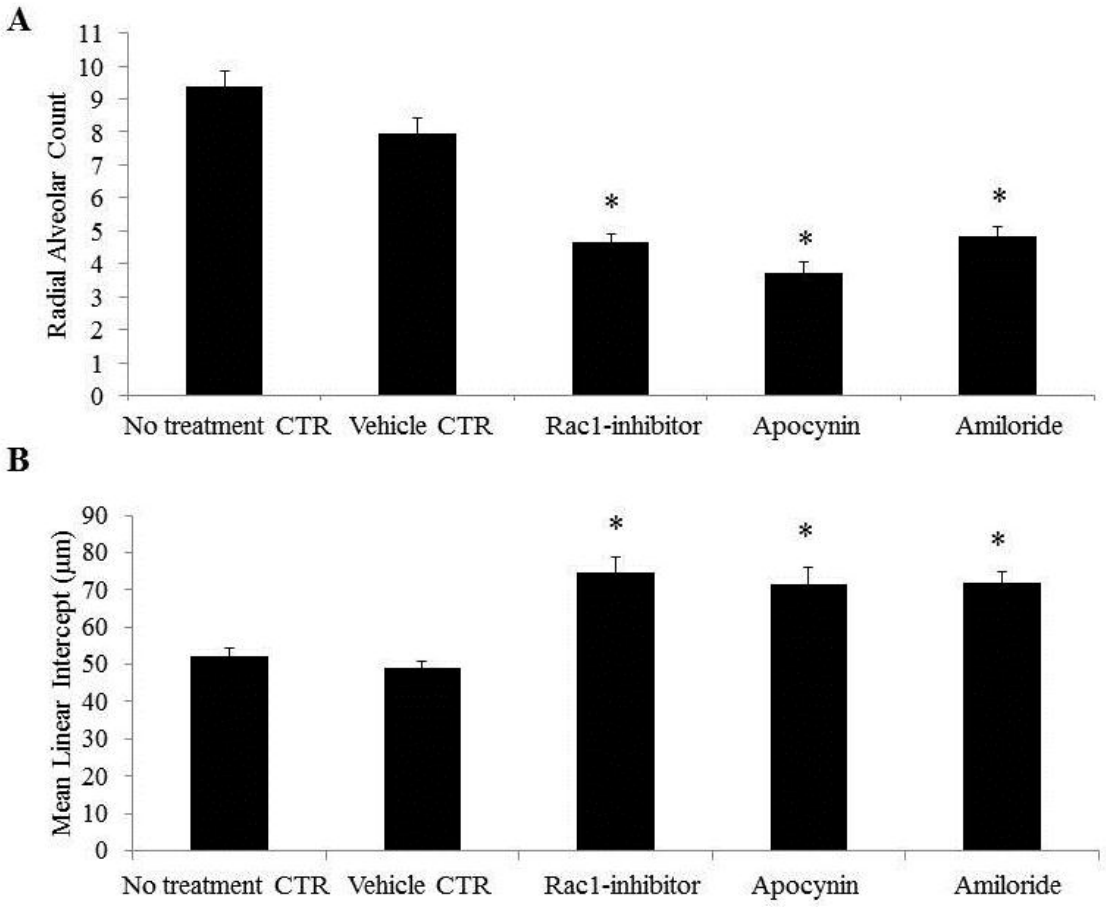


*Figure 11. ENaC, Rac1, and Nox inhibitors obstruct lung alveolarization.*

P15 mouse pups exposed to NSC 23766, amiloride, or apocynin, inhibitors of Rac1, Nox, and ENaC activity, respectively, demonstrate a reduction in radial alveolar count compared to vehicle control (*A*) and an increase in mean linear intercept (*B*). No treatment control group: $N = 35$ independent observations from 2 mice. Vehicle control group: $N = 29$ independent observations from 2 mice. Rac1-inhibitor treatment group: $N = 36$ independent observations from 3 mice. Apocynin treatment group: $N = 10$ independent observations from 1 mouse. Amiloride treatment group: $N = 40$ independent observations from 3 mice. $^*P < 0.05$ compared to vehicle.

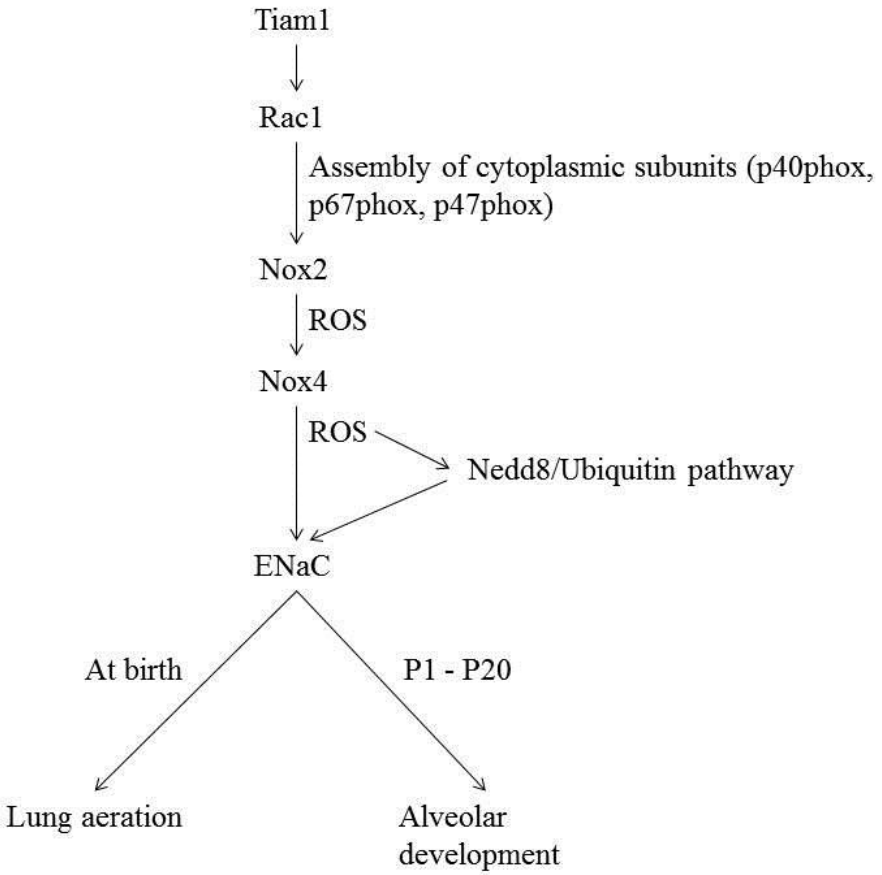


*Figure 12. Schematic of proposed signaling pathway for lung aeration and alveolar development in neonatal mice*